J. Phys. D: Appl. Phys. **31** (1998) 3349–3357. Printed in the UK PII: S0022-3727(98)94852-5

Rf breakdown of low-pressure gas and a novel method for determination of electron-drift velocities in gases

V A Lisovskiy† and V D Yegorenkov‡

† Department of Physics and Technology, Kharkov State University, 4 Svobody Square, 310077, Kharkov, Ukraine
‡ Department of Physics, Kharkov State University, 4 Svobody Square, 310077, Kharkov, Ukraine

Received 3 June 1998

Abstract. This paper reports the results of the detailed and comprehensive experimental and theoretical treatment of the rf gas breakdown. We give the measured breakdown curves of the low-pressure rf discharge in argon, hydrogen and air in a broad range of gas pressures and interelectrode distances. The different processes of generation and loss of charged particles participating in the rf gas breakdown are discussed. We suggest to distinguish the following sections on the rf discharge breakdown curves: multi-pactor, Paschen, diffusion-drift and emission-free ones. The analytic gas breakdown criterion of the combined (rf plus weak dc electric field) discharge taking into account the anisotropy of electron diffusion in the electric field is obtained. A novel method for determining the electron-drift velocity from the measured rf breakdown curves is suggested. The electron-drift velocity data in argon, hydrogen and air obtained with this technique in the range $E/p \approx 50$–2000 V cm^{-1} Torr^{-1} are given and compared with those got by conventional means.

1. Introduction

Radio frequency (rf) capacitive gas discharge is widely employed in various technological processes such as plasma etching of semiconductor materials [1, 2], deposition of diamond-like thin films [3, 4] and pumping of gas lasers [5]. To optimize plasma technological processes it is often necessary to know the conditions of gas breakdown in a discharge device [6]. Therefore experimental measurements and numerical simulations of breakdown curves of a discharge in a uniform rf field are of considerable interest.

Our paper consists of two parts. The first one deals with gas breakdown in rf and combined (rf plus dc) electrical fields. The second one is devoted to determination of the electron-drift velocity using the peculiarities of breakdown curves.

We have already made an attempt to outline some of the previous work in this field several years ago in the framework of a phenomenological approach [7]. However, the latest developments dealing with a detailed pattern of particle diffusion together with a deeper study of the work done have induced us to try once again to do it from the point of view of the approach presented.

Let us present a brief survey of papers devoted to the rf gas breakdown and of the results obtained in them. Gutton *et al* [8] recorded the rf breakdown curves in air in a discharge vessel with external plane electrodes in the frequency range 50 Hz to 2 MHz. Kirchner [9] developed in detail the technique of recording breakdown curves in a rf field. However, the author of [9] failed to construct rf breakdown curves because of the large spread of measured values of the breakdown voltage and gave his results in the form of a table. Gutton and Gutton [10] obtained the breakdown curves of the rf discharge in hydrogen in a broad frequency range (53 kHz to 96 MHz). Gutton [11] recorded a large number of breakdown curves in long tubes with external hollow electrodes in hydrogen and oxygen and also discovered a discontinuity in the dependence of the rf breakdown voltage on the wavelength with fixed pressure. Gill and Donaldson [12] observed rf breakdown curves with two minima. Thomson [13] developed an elementary theory of rf gas breakdown and also obtained similar breakdown curves in hydrogen. Zouckermann [14] measured breakdown curves in discharge tubes with external electrodes and clarified the effect of mercury vapour on the shape of breakdown curves. Githens [15] and Chenot [16] obtained a vast amount of rf breakdown curves in hydrogen in discharge vessels of various forms in broad ranges of gas pressure and frequency. Hale [17] also proposed a simple theory explaining the mechanism of gas breakdown in an alternating electrical field. Pim [18] recorded the rf breakdown curves in air in the frequency range 100–300 MHz with inter-electrode gaps less than

1 mm. Gill and Engel [19], Harris and Engel [20] and Francis [21] studied the dependence of the rf field's breakdown value on the wavelength of the electrical field applied at fixed values of the gas pressure.

Kihara [22] gave a kinetic treatment of processes occurring in rf electrical discharges in gases and obtained a condition for gas breakdown in a uniform rf field in a diffusion regime. However, the obtained equation for the gas breakdown in the rf field gave an unsatisfactory description of the recorded breakdown curves [15]. Salmon [23], starting from the work by Kihara [22], obtained an analytical expression for the electron distribution function over velocities in the rf field and made some remarks concerning the role played by the secondary electron emission in the rf gas breakdown [24]. In an attempt to improve the agreement between the theory [22] and experiments [15] Sen and Ghosh [25] suggested that one should determine numerical values of molecular constants used in [22] from experimental data rather than from the form of the models adopted in [22]. However, this did not give a considerable improvement.

Levitskii [26] showed both in theory and by experiment that there is a region of multi-valued dependence of the rf breakdown voltage U_{rf} on the gas pressure p to the left of the minimum of rf breakdown curves. Kropotov *et al* [27, 28] have measured the rf breakdown curves in various gases with various schemes for connecting an rf generator to the discharge electrodes. Lisovskiy and Yegorenkov [29] have obtained approximate formulae describing various sections of recorded rf breakdown curves. From the recorded breakdown curves [7] they have determined values for the molecular constants used by Kihara [22] with which Kihara's equation fits the measured curves best and have studied the influence of a longitudinal dc electrical field on the rf breakdown of gases [7, 30]. The problem of the effect of the dc electrical field on the rf discharge breakdown (ignition of the longitudinal combined discharge) had previously been studied in papers by Kirchner [9, 31], Pim [18], Levitskii [26], Varela [32] and Sen and Bhattacharjee [33, 34]. The effect of the electrode material on the rf breakdown has been studied both in theory and by experiment in [35, 36]. Thompson and Sawin [37] have performed numerical and experimental studies of rf breakdown in SF_6. Sato and Shoji [38] have recorded the right-hand sides of rf breakdown curves in argon and obtained the analytical condition for the rf breakdown accounting for the anisotropy of the electron diffusion (the difference between the coefficients of longitudinal and transverse diffusion of electrons).

This paper reports the rf breakdown curves measured in air, argon and hydrogen in a broad range of gas pressures and inter-electrode gaps. Also the analytical criterion for the gas breakdown in the combined (rf plus dc) electrical field is obtained accounting for the anisotropy of the electron diffusion in the electrical field. We predict the existence of the multi-valued region from the dependence of the rf breakdown field on the wavelength of the applied electrical field.

This multi-valued region is very convenient to use for the determination of the drift velocity of electrons V_{dr} that is one of the basic parameters describing the motion of electrons in a gas under the influence of an electrical field because it is dominant in characterizing the electrical conductivity of a weakly ionized gas. Several techniques to measure the electron drift velocity (a time-of-flight technique, a technique registering the optical radiation of a moving electron swarm, a shutter technique and so on) have been developed. Detailed descriptions of these techniques and results obtained with them may be found, for example in [39, 40]. These techniques, as a rule, permit one to determine the electron drift velocities in the range $E/p \leq$ 200–300 V cm^{-1} Torr^{-1}. At higher values of the quantity E/p a self-sustained discharge ignites between the electrodes of the experimental device and it becomes difficult to measure the electron drift velocity with conventional means [39].

We suggest a method for determining the electron drift velocity values from the recorded rf breakdown curves. With this method we have obtained the electron drift velocity values in the range $E/p \approx$ 50–2000 V (cm^{-1} Torr^{-1}). Whereas in other techniques ignition of the discharge is undesirable, the method for the determination of the electron drift velocity suggested in this paper is based precisely on studying the electrical breakdown of a gas.

2. Experimental details

Rf gas discharges have been ignited in argon, air and hydrogen within the pressure range $p = 10^{-2}$–20 Torr with the rf field frequency $f = 13.56$ MHz. The discharge gap between planar round stainless steel electrodes has been varied within the range $L =$ 6.5–70 mm. As a rule, the electrodes' diameter was 100 mm but several rf breakdown curves have been recorded for discharge tubes with inner diameters 5, 13 and 20 mm. The rf voltage's amplitude has been varied within the range $U_{rf} =$ 0–1000 V.

The rf voltage has been applied to one of the electrodes while the other one has been grounded. A choke of 4 mH has connected the electrodes in order to remove the dc bias voltage. We have not used any external ionization sources and have studied exclusively the ignition of self-sustained rf discharges.

We have employed the technique of recording rf breakdown curves suggested by Levitskii [26]. Near to and to the right-hand side of the breakdown curve minimum we have fixed a certain value of the gas pressure and increased the rf voltage across the electrodes slowly until breakdown of the discharge occurs. In the region of the multi-valued dependence of the rf breakdown voltage (the left-hand side of the breakdown curve) we have fixed a certain rf voltage at a sufficiently low pressure ($p \simeq 10^{-3}$–10^{-2} Torr) and then the pressure in the vessel has been increased slowly until the discharge ignites.

Rf voltage from the nongrounded electrode has been fed to the phase-difference meter (FK2-12) via a capacitance divider. The rf current has been measured with a Rogowski coil whose signal has also been fed to the FK2-12 device. This has permitted us to obtain the amplitudes of the rf voltage and current together with the phase shift φ between

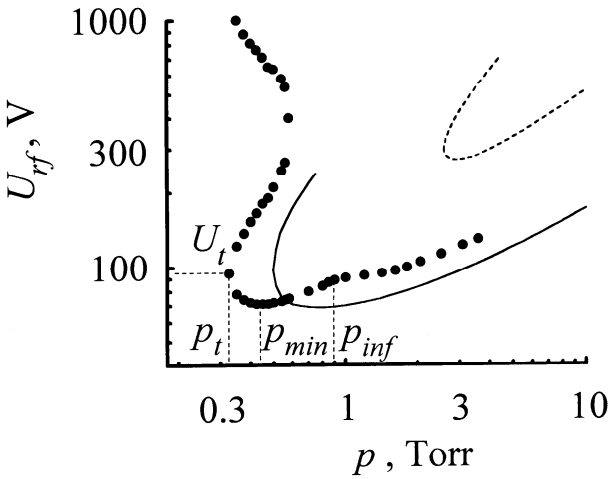

Figure 1. Curves for rf breakdown in hydrogen at L = 20 mm: dots present our measured data, the full curve is calculated according to equation (4) and the broken curve is calculated according to Kihara's equation [22].

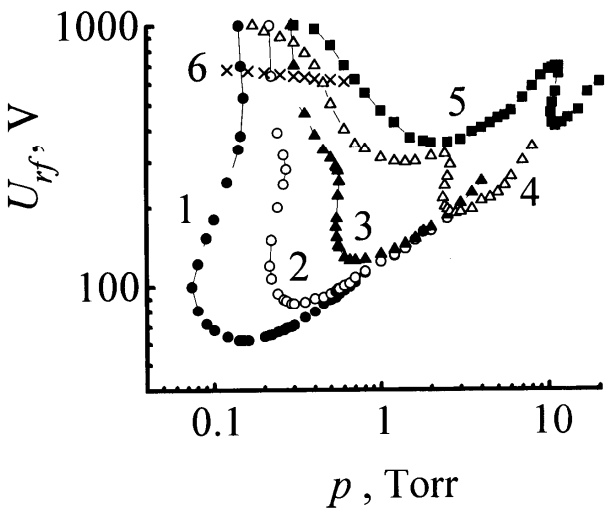

Figure 2. Curves for RF breakdown in air: 1, L = 29 mm; 2, L = 20 mm; 3, L = 14 mm; 4, L = 9 mm; 5, L = 6.5 mm; and 6, the breakdown curve for a dark rf discharge at L = 6.5 mm.

them. In the absence of the rf discharge the phase shift was $\varphi = \pi/2$. The appearance of the ohmic current in the discharge circuit ($\varphi < \pi/2$) and the light in the discharge vessel have indicated the occurrence of gas breakdown.

The inaccuracy of measuring the rf breakdown voltage U_{rf} was ± 2 V within the range $U_{rf} \leq 500$ V and ± 5 V within the range $U_{rf} > 500$ V. The breakdown time lag has not exceeded 1–5 s within the total ranges of gas pressure and rf voltage being studied.

3. Discussion of recorded curves of rf discharge breakdown

As we have already said, there is a range for which there is a multi-valued dependence of the breakdown voltage U_{rf} on the gas pressure p in the low-pressure region to the left-hand side of the breakdown curve's minimum. Figure 1 shows a characteristic breakdown curve of a rf discharge in hydrogen. Figure 1 also shows such points as a turning point (at the pressure $p = p_t$ and rf voltage $U_{rf} = U_t$), a minimum point and an inflection point (at $p = p_{inf}$ and $U_{rf} = U_{inf}$). One can deduce the U_{inf} and p_{inf} values from those for U_{min} and p_{min} according to the relations [7]

$$\frac{U_{inf}}{U_{min}} = \frac{\mathrm{e}}{2} \qquad \frac{\mathrm{e}}{2} < \frac{p_{inf}}{p_{min}} < \mathrm{e}$$

where e is the base of natural logarithms.

One can divide breakdown curves into several characteristic sections differing with regard to the processes participating in the rf gas breakdown. For example the branch of the breakdown curve to the right-hand side of the inflection point ($p > p_{inf}$) [27] depends weakly on the electrode material [7, 35, 36]; therefore, one can assume that, at $p > p_{inf}$, the secondary electron emission from electrode surfaces does not participate in the rf gas breakdown. Hence we will call this part of the rf breakdown curve an emission-free branch. A so-called diffusion–drift branch of the rf breakdown curve exists in the pressure range between the turning point and an inflection point. In this case the secondary emission from electrodes does participate in the rf breakdown together with the ionization of gas molecules via electron impact, electron drift in the rf field and losses of electrons on the surfaces of electrodes and vacuum-vessel walls. The improvement of emission properties of electrodes' surfaces leads to a decrease of the rf breakdown voltage values and to a shift of the rf breakdown curve to the region of lower pressures. The diffusion–drift branch is most pronounced for sufficiently large inter-electrode gaps ($L > 1$ cm) (figures 1–3). With smaller gaps ($L < 1$ cm) it is less pronounced but a second minimum might be observed (figure 2). This second minimum is located at pressures lower than those for the minimum of the diffusion–drift branch and it is sometimes called a basic (Paschen) minimum [41]. Therefore we will also tentatively call the corresponding branch of the rf breakdown curve a Paschen one (it was called a secondary-emission branch in [29] and b-mode breakdown in [15]). Below we will give our reason why this branch of the breakdown curve should be called a Paschen one.

Now we will consider the processes participating in the rf gas breakdown in more detail by adopting Townsend's conception of an average electron. Take a point on the breakdown curve at $p > p_{inf}$. A rf discharge is ignited when electrons gain the energy required for ionizing gas molecules. Besides, the number of electrons born due to ionization should be equal to the number of electrons lost due to the oscillatory motion in the rf field and by diffusion to the electrodes and vacuum-vessel walls. The amplitude of the electrons' displacement in the rf field $A = eE_{rf}/(m\nu_{en}\omega)$ (E_{rf} is the amplitude of the rf field, e and m are the electron's charge and mass, respectively, $\omega = 2\pi f$ and ν_{en} is the frequency of electron–neutral species collisions) in this pressure range is small compared with the inter-electrode gap L. Raizer [42] claims that, for a discharge to break, every electron should perform on average 3–10 ionizing collisions with gas molecules before

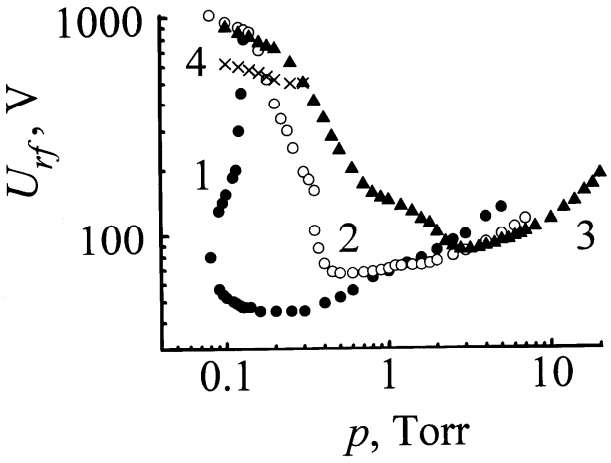

Figure 3. Curves for rf breakdown in argon: 1, L = 23 mm; 2, L = 13 mm; 3, L = 6.5 mm; and 4, the breakdown curve for a dark rf discharge at L = 6.5 mm.

being lost on the vessel walls or electrodes. This is probably true for a dc gas breakdown as well as for a rf one.

Let us now decrease the gas pressure in the discharge vessel a little. The electron collides with gas molecules not so frequently, so its energy losses for the excitation of electronic, vibrational and rotational levels of molecules are not as large. Therefore it can gain the energy necessary for the ionization of molecules in a weaker rf field and the rf breakdown voltage decreases with decreasing pressure.

For gas pressures $p \leq p_{inf}$ the secondary electron emission from electrode surfaces begins to play a role in rf gas breakdown [7, 35, 36]. A fraction of electrons that are lost on the electrodes due to the oscillatory motion in the rf field may return to the inter-electrode gap in the form of secondary electrons. This means that an additional source of charged particles participates in the rf breakdown. Therefore the rf breakdown voltage decreases faster with decreasing gas pressure for $p \leq p_{inf}$ than it does for $p > p_{inf}$.

The further decrease of the gas pressure has as a consequence a noticeable loss of electrons to the electrodes due to the oscillations in the rf field. Therefore the rf breakdown voltage approaches a minimum (for a diffusion–drift branch) and then starts to increase. When the condition $A \approx L/2$ is satisfied, many electrons are lost to the electrodes and the breakdown curve passes through a turning point with the coordinates $p = p_t$ and $U_{rf} = U_t$ (figure 1).

Now let us establish the pressure $p = p_t$ in the discharge vessel and apply across the electrodes a rf voltage that is slightly above U_t. Under these conditions the rf discharge may not ignite because the electrons are mostly lost to the electrodes, having no time to perform a sufficient number of ionizing collisions. To ignite a rf discharge one should apply high rf voltages across the electrodes that permit electrons to gain high energies (tens of electron-volts). Then the rate of ionizing collisions of electrons with gas molecules increases sharply, together with the secondary electron emission resulting from collisions of electrons with electrode surfaces. Another way of igniting a discharge consists of increasing the gas pressure, namely providing a large number of gas molecules on the paths of electrons going to the electrodes. Therefore the rf breakdown curve is deflected towards the region of higher gas pressures and we can observe the region of the multi-valued dependence of the rf breakdown voltage on the gas pressure.

The further qualitative behaviour of the rf breakdown curve depends strongly on the inter-electrode gap's width and the nature of the gas. With small gaps the diffusion–drift branches are located at sufficiently high pressures ($p \approx$ 2–10 Torr) (see, for example, rf breakdown curves in air at L = 6.5 and 9 mm in figure 2). One clearly observes the multi-valued region of the rf breakdown curve in air for practically the whole range of gaps L we have studied. If the amplitude of the electrons' displacement in the rf field exceeds the inter-electrode gap, $A \geq L$, then the gas breakdown in the rf field evolves similarly to the one in the dc field with the electrical field's polarity changing every half period. The considerable amount of electrons travelling from an instantaneous 'anode' to an instantaneous 'cathode' happens to gain substantial energy for performing ionizing collisions with gas molecules. If the inter-electrode gap's width and the gas pressure are such that the ionization capacity of electrons rises with lowering of the pressure, then the second minimum on the rf breakdown curve (corresponding to a Paschen branch) appears. Thus our reason for calling this branch a 'Paschen' one is based on the similarity between the rf breakdown under these conditions and dc breakdown. On lowering the pressure the ionization capacity of electrons approaches a maximum and then decreases. The rf breakdown voltage passes through the second (Paschen) minimum and then grows. The rf breakdown curves for argon (figure 3) exhibit the multi-valued region only with sufficiently large inter-electrode gap widths ($L \geq$ 15 mm). Voltages for rf breakdown in argon are noticeably lower than those for air and for hydrogen. On rf breakdown curves for argon we have observed only one minimum corresponding to the diffusion–drift branch throughout the studied range of gap widths. It was located at lower pressures than the similar minimum for breakdown in air. For example, with the gap width L = 6.5 mm we have $p_{min} \approx$ 3 Torr in argon and $p_{min} \approx$ 12 Torr in air.

At a sufficiently low gas pressure the rf breakdown voltage depends weakly on the gas pressure (figures 2 and 3). Probably we observe here a transition to a resonant rf breakdown regime governed by secondary emission [43–47]. This branch of the rf breakdown curve is often called a multi-pacting one. At low pressures electrons move along the discharge vessel colliding with the electrodes much more often than they collide with gas molecules. Electrons can multiply themselves only if they move to and fro between the electrodes in resonance with the field and hit the walls hard enough to eject secondary electrons.

Figures 2 and 3 show the rf voltage values under which the phase shift φ becomes less than $\pi/2$ with L = 6.5 mm. With the rf voltage increasing the phase shift decreases (to as little as $\pi/6$) and weak blue light visible to the naked eye appears in the vessel, filling the whole of the

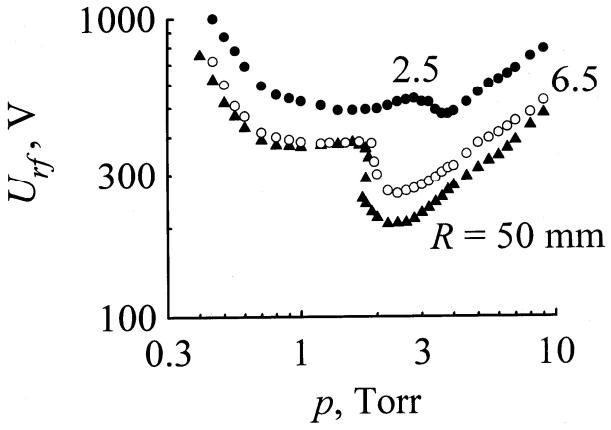

Figure 4. Curves for rf breakdown in air at L = 1 cm with the following radii of the discharge tube: R = 50, 6.5 and 2.5 mm.

inter-electrode gap uniformly. On further increasing the rf voltage a self-sustained rf discharge with a characteristic structure (electrode sheaths near each electrode) ignites, the rf discharge in air being pink in colour. One observes a similar phenomenon in all gases we have studied. Perhaps the weak blue light observed at low pressures and with small gaps relates to the dark (silent) rf discharge preceding the ignition of the self-sustained rf discharge. For large gaps ($L > 1$ cm) this dark rf discharge is not observed throughout the ranges of gas pressures and rf voltages being studied.

The authors of [41–43] claim that the condition $\omega \approx \nu_{en}$ is satisfied at the minimum of the Paschen branch. Consider the breakdown curve for $L = 6.5$ mm presented in figure 2. The Paschen minimum is located at $p \approx 2.5$ Torr. At this pressure the rate of electron–neutral species collisions is $\nu_{en} \approx 9.8 \times 10^9$ s^{-1} [42]. For the rf generator used in this work the linear frequency is $f = 13.56$ MHz and the angular frequency is $\omega \approx 8.5 \times 10^7$ s^{-1}. Therefore one can state that the condition $\omega \ll \nu_{en}$ is satisfied at the minimum of the Paschen branch of the rf breakdown curve. The same conclusion also follows from other breakdown curves obtained in this paper as well as, for example, in [11, 15, 16].

Now consider the influence of the discharge vessel's diameter on the shape of the rf breakdown curve (figure 4). When the discharge vessel's diameter exceeds the inter-electrode gap considerably, we observe the pronounced diffusion–drift branch with the multi-valued region as well as a section near and to the left-hand side of the minimum of the Paschen branch. On decreasing the electrodes' diameter the multi-valued region disappears and the diffusion–drift branch is shifted towards the region of higher pressures and rf voltages, the Paschen branch changing slightly. When the electrodes' diameter becomes substantially less than the inter-electrode gap, we observe a considerable increase of the rf breakdown voltages in the whole range of gas pressures studied, this being due to the sharp increase of electron losses. The diffusion–drift branch becomes less pronounced. The results we have obtained (figure 4) are in good agreement with the results of [16].

4. The criterion for breakdown in a combined electrical field

The work by Kihara [22] is one of the first papers devoted to a consistent theoretical treatment of the diffusion–drift branch of the rf breakdown curve. The criterion for the rf gas breakdown obtained in this work has included the elastic and inelastic (exciting and ionizing) collisions of electrons with gas molecules. It has also included the isotropic diffusion of electrons to the electrodes and discharge-vessel walls as well as the oscillating motion of the electron cloud in the rf field. Kihara has described the elastic, exciting and ionizing collisions of electrons with gas molecules with the help of a set of molecular constants depending on the gas species. However, the rf breakdown criterion obtained by Kihara [22] does not agree satisfactorily with recorded breakdown curves. Figure 1 shows the curve for rf breakdown in hydrogen that we have measured as well as the curve calculated according to Kihara's theory with the molecular constants given in [22]. The reasons for the disagreement between Kihara's calculations and measured data are probably the following. First, Kihara neglected the emission of secondary electrons from electrode surfaces while deriving his rf breakdown criterion. Second, Kihara assumed the electron-diffusion coefficient to be directly proportional to the rf field's intensity, $D_e \propto E_{rf}$. Actually, the electron-diffusion coefficient D_e is a complicated function of the ratio of the electrical field's intensity and the gas pressure E/p [48–53]. Therefore the relationship $D_e \propto E_{rf}$ does not hold generally. Third, Kihara assumed the electron diffusion to be isotropic. However, in later papers [39, 54–58] it has been shown that, as a rule, the coefficient for diffusion of electrons along the direction of the electrical field D_L is not equal to the one for their diffusion across the electrical field D_e, that is, the diffusion of electrons is anisotropic. For example, for argon at $E/p \approx 50$ V cm^{-1} Torr^{-1} $D_e p \approx 2 \times 10^6$ cm^2 Torr s^{-1} and $D_L p \approx 10^6$ cm^2 Torr s^{-1}, that is, $D_e/D_L \approx 2$. As the diffusion of electrons to the electrodes and vessel walls plays a substantial part in rf gas breakdown, obviously, one should take the anisotropy of the electrons' diffusion into account when deriving the criterion for rf gas breakdown [38].

In this section we will obtain the criterion for gas breakdown in combined (rf plus weak dc) electrical fields. Consider a discharge gap between planar electrodes spaced L apart, the electrodes' radius being R. It is equal to the discharge tube's radius. Let a rf field E_{rf} and a weak dc electrical field E_{dc} (not contributing to gas ionization) be applied simultaneously across the electrodes. Let the z axis be directed normal to the electrodes' surfaces and the radial coordinate r be calculated along the electrodes' surfaces, the origin of coordinates being located at the centre of the discharge gap.

The balance equation for electrons is written in the form

$$\frac{\partial n_e}{\partial t} = \nu_i n_e + D_e \frac{1}{r}\frac{\partial}{\partial r}\left(r\frac{\partial n_e}{\partial r}\right) + D_L \frac{\partial^2 n_e}{\partial z^2} - V_e \frac{\partial n_e}{\partial z}\cos(\omega t) - V_{dc}\frac{\partial n_e}{\partial z} \qquad (1)$$

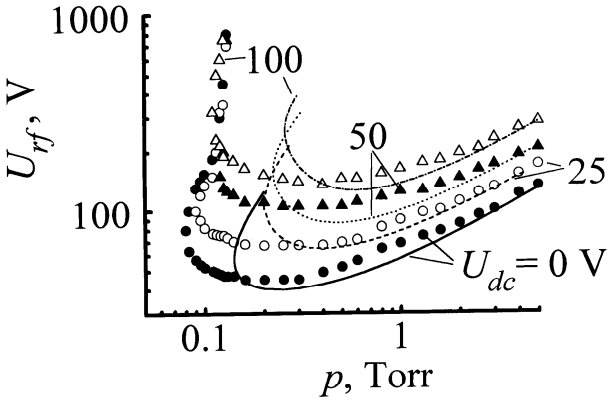

Figure 5. Rf breakdown curves of a longitudinal combined discharge (rf plus weak dc electrical fields) for the following dc voltage values: U_{dc} = 0, 25, 50 and 100 V. Points depict the measured data from [7]; curves are calculated according to equation (4).

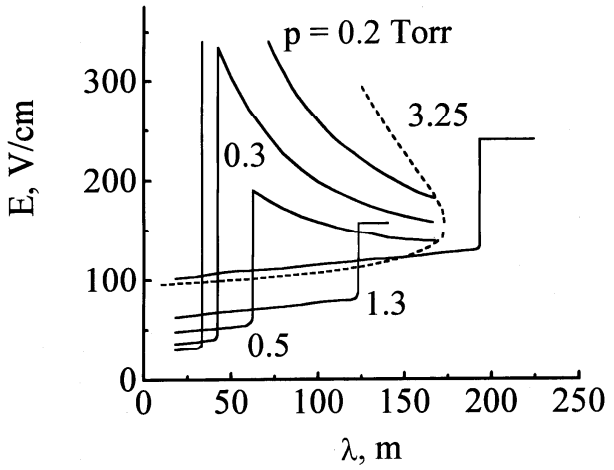

Figure 6. The breakdown rf field in hydrogen against the rf field's wavelength: the full curve depicts the measured data from [19] for the pressure values p = 0.2, 0.3, 0.5, 1.3 and 3.25 Torr; the broken curve is calculated according to equation (4) (p = 3.25 Torr).

where n_e is the electron density, ν_i is the rate of ionization of gas molecules via the impact of electrons, D_e and D_L are the coefficients of transverse and longitudinal diffusion, respectively, $V_e = eE_{rf}/(m\nu_{en})$ and $V_{dc} = eE_{dc}/(m\nu_{en})$.

The boundary conditions are written in the form

$$n_e(R, z) = 0 \tag{2}$$

$$n_e\left(r, \pm\frac{L}{2}\right) = 0. \tag{3}$$

The separation of variables in a steady state yields the criterion for the gas breakdown in the rf and weak dc electrical fields (a longitudinally combined electrical field):

$$\frac{\nu_i}{D_e} = \left(\frac{2.4}{R}\right)^2 + \frac{D_L}{D_e}\frac{\pi^2}{[L - (2V_e/\omega)]^2} + \frac{V_{dc}^2}{4D_eD_L}. \tag{4}$$

In the absence of the dc electrical field we get from (4) the criterion for rf gas breakdown [38]. When the electrons' diffusion is isotropic ($D_e \approx D_L$) and the electrodes are infinitely large, equation (4) transforms to the criterion for rf gas breakdown obtained by Kihara [22].

Figures 1 and 5, respectively, compare the breakdown curves calculated from the criterion (4) with measured breakdown curves of the rf and longitudinally combined discharges. In calculations we have used the values of V_e, D_L and D_e given in [48–52, 59–66] and, to obtain the ionization rate $\nu_i = \alpha V_e$, we have taken values of the first Townsend coefficient from [42, 62, 65–67].

Figures 1 and 5 show that there is satisfactory agreement between the curves calculated from equation (4) and the measured ones in the region near and to the right-hand side of minima of breakdown curves, the calculated curves being located in regions of higher gas pressures than are the measured ones. Perhaps this difference is caused by the secondary electron emission from the electrode surfaces not being included in our derivation of equation (4). As was shown in [35, 36], the breakdown curves for non-emitting electrodes (calculated curves in our case) are located in regions of higher pressures than those for the electrodes whose surfaces emit secondary electrons.

As one can see from figures 1 and 5, the calculated curve for the diffusion–drift branch is a two-valued one (apart from the turning point), permitting one to describe the multi-valued dependence of the breakdown rf voltage on the gas pressure.

As we have already said, Gutton [11], Gill and Engel [19], Harries and Engel [20] and Francis [21] studied the dependence of the breakdown voltage of the rf discharge in cylindrical glass vessels on the frequency of the applied field. Figure 6 shows some recorded breakdown curves [19] for hydrogen. Gill and Engel [19] established a certain value of the gas pressure and measured the rf field breakdown values for various wavelengths of the rf field. At all pressures a sharp discontinuity in the breakdown field's behaviour on increasing the wavelength has been observed. The authors of [19] related the appearance of the discontinuity to the fact that the amplitude of electrons' oscillations in the rf field becomes approximately equal to the half width of the inter-electrode gap for the given wavelength λ_b and a fixed pressure, leading to a sharp increase of electron losses. Obviously, a sharp increase of the rf breakdown field with the gas pressure fixed and the wavelength $\lambda = \lambda_b$ [11, 19–21] is essentially similar to a sharp increase of the rf breakdown voltage with the wavelength fixed and the gas pressure $p = p_t$ (figures 1–4). In both cases the sharp increase of the rf breakdown field occurs when the condition $A \approx L/2$ holds. In [15, 16] one has actually observed a sharp increase of the rf breakdown voltage on all breakdown curves. Only Levitskii [26] has shown the existence of the multi-valued dependence on rf breakdown curves and explained the observed discontinuity as a sharp transition from the turning point of the diffusion–drift branch at $p = p_t$ and $U_{rf} = U_t$ to the section of the rf breakdown curve that we call a Paschen branch.

Because the criterion (4) predicts successfully the existence of the multi-valued region of the dependence $U_{rf}(p)$, let us check the possibility of predicting the multi-valued region of the dependence $E_{rf}(\lambda)$ with p = constant

[19]. Figure 6 presents the results of such calculations for the pressure of hydrogen $p = 3.25$ Torr. The calculated curve in figure 6 is a two-valued one. Therefore a plausible guess is that Gill and Engel [19] could have observed the multi-valued region of the dependence $E_{rf}(\lambda)$ with the following technique. Establish the wavelength value $\lambda > 200$ m and fix the rf field value (for example, at $E_{rf} = 200$ V cm^{-1}) and increase the wavelength smoothly. Thus the criterion for rf breakdown (4) predicts successfully the multi-valued regions both of the $U_{rf}(p)$ and of the $E_{rf}(\lambda)$ dependences.

5. Determining the electron drift velocity from breakdown curves of rf discharges

In many problems describing electrons' motion in a strong electrical field (such as, in a cathode sheath of a dc discharge and in an electrode sheath of a rf discharge) one should know the electrons' drift velocity V_{dr} at large values of the ratio of the electrical field strength to the gas pressure E/p. As we have already said, conventional techniques [39, 40] permit one to measure electron-drift velocities in the range $E/p \leq 200$–300 V cm^{-1} Torr^{-1}. If one attempts to create a stronger electrical field in an experimental device, a self-sustained discharge may ignite, impeding substantially the measurements of the electron-drift velocity. It is only natural to try to estimate the drift-velocity values at large E/p from the measured breakdown curves.

As far as we know, Gill and Engel [19] were the first to make such an attempt. They estimated the electron-drift-velocity values from the position of the discontinuity of the dependence $E_{rf}(\lambda)$ and the value of the rf field at this point. The electron-drift velocity is proportional to $\sqrt{E}$ at large E/p, therefore it may be written as

$$V(t) = \frac{\mathrm{d}x}{\mathrm{d}t} = K[E_{rf}\sin(\omega t)]^{1/2} \tag{5}$$

where K is a constant factor [43]. If one takes double the amplitude of the electrons' oscillations in the rf field equal to the inter-electrode gap's width, then one gets

$$\frac{L}{1.2} = 2K\frac{\sqrt{E_{rf}}}{\omega}. \tag{6}$$

Consequently, from the measured limiting wavelength $\lambda_b = 2\pi c/\omega$ and the amplitude value of E_{rf} at the bottom of the discontinuity, one can obtain the value of K and the electron-drift velocity V_{dr} corresponding to the amplitude value E_{rf}/p. Figure 7 shows the electron-drift-velocity values for hydrogen obtained with this technique that are in good agreement with the results obtained with conventional techniques [48–51].

A disadvantage of such a technique of determining V_{dr} is that one requires a sufficiently powerful rf generator to provide smooth control of the rf field's frequency (in a broad range of wavelengths) while keeping the rf voltage across the electrodes of the experimental device constant. The rf generators that are being industrially manufactured nowadays possess the admissible frequency

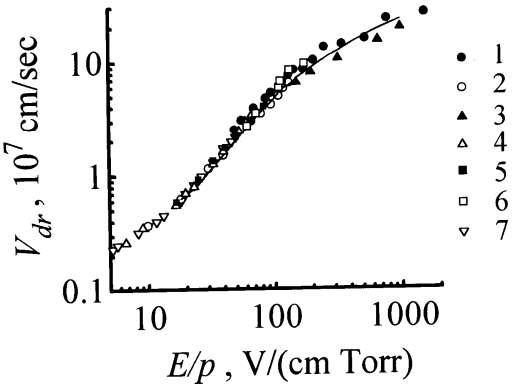

Figure 7. The electron-drift velocity in hydrogen against E/p: 1, our results and 2–7, other measured data (2 is from [60], 3 is from [68], 4 is from [62], 5 is from [69], 6 is from [19], 7 is from [70] and the curve is calculated in [60]).

$f = 13.56$ MHz (and its higher harmonics), thus presenting an additional obstacle. Therefore we suggest the following changes to the technique for measuring the electron-drift velocity given in [19].

As can be seen in figure 1, on rf breakdown curves one observes a turning point with the coordinates $p = p_t$ and $U_{rf} = U_t$. This point is pronounced and the amplitude of the drift displacement of electrons in the rf field is equal here to $A \approx L/2$ [26]. Therefore we suggest in this paper that one should determine the electron-drift velocity using the position of the turning point of the breakdown curve of the rf discharge.

Measured and calculated data [48, 50, 60] show that two characteristic sections are observed for the dependence of the electron-drift velocity on the quantity E/p in the presence of inelastic electron–neutral collisions. For example, for hydrogen with $E/p \approx 10$–200 V cm^{-1} Torr^{-1} the electron-drift velocity is proportional to E/p ($V_{dr} \propto E/p$) whereas at $E/p > 200$ V cm^{-1} Torr^{-1} we observe the root dependence $V_{dr} \propto (E/p)^{1/2}$.

Consider the electrons' motion in the uniform rf field. The electron-drift velocity in a rf field that is not very strong (with $E/p < 200$ V cm^{-1} Torr^{-1}) can be written in the form (at $\nu_{en} \gg \omega$)

$$V(t) = \frac{eE_{rf}}{m\nu_{en}}\cos(\omega t). \tag{7}$$

The amplitude value of the drift velocity is a maximum instantaneous electron velocity corresponding to the maximum value of the rf field strength. Integrating (7) over time yields the amplitude of the electrons' displacement in the rf field

$$A = \frac{eE_{rf}}{m\nu_{en}\omega} = \frac{V_{dr}}{\omega}. \tag{8}$$

On decreasing the gas pressure the amplitude of the electrons' displacement increases and the condition $A \approx L/2$ is satisfied at the first turning point of the rf breakdown curve with $p = p_t$ and $U_{rf} = U_t$. Thus, for the electron-drift velocity we have

$$V_{dr} = L\pi f. \tag{9}$$

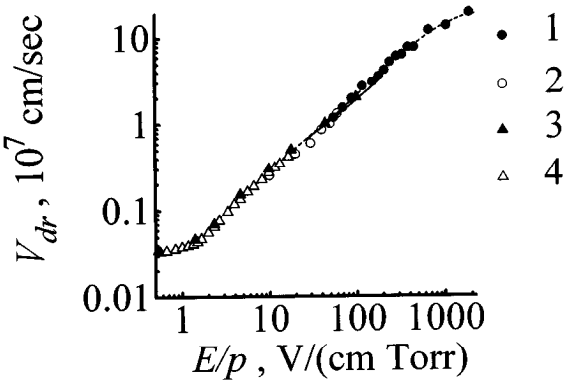

Figure 8. The electron-drift velocity in argon against E/p: 1, our results and 2–4, other measured data (2 is from [71], 3 is from [50], 4 is from [52], the full line is calculated in [59] and the broken line is calculated in [50]).

With the rf field's frequency and the inter-electrode gap fixed, the electron-drift-velocity value is constant at the first turning point of the rf breakdown curve and it does not depend on the nature of the gas. The coordinates of the turning point permit one to calculate the ratio E/p related to the obtained value of the electron-drift velocity. For example, figure 1 gives for the coordinates of the first turning point the values $p_t = 0.32$ Torr and $U_t = 95$ V; consequently, $E/p = U_t/(p_t L) \approx 147$ V cm^{-1} Torr^{-1}. The electron-drift-velocity value for $L = 2$ cm is $V_{dr} = 8.5 \times 10^7$ cm s^{-1}.

For strong electrical fields ($E/p > 200$ V cm^{-1} Torr^{-1}) one gets easily from (6) that

$$V_{dr} = L\pi f/1.2. \tag{10}$$

One sees from (9) and (10) that the technique of determining the electron-drift velocity from the location of the first turning point is weakly sensitive to the power of the dependence of V_{dr} on E/p.

It has been assumed in equations (5)–(10) that $\nu_{en} \gg \omega$; that is, during the rf field period electrons collide many times with gas molecules. This assumption is valid for our measurements because even for $L = 70$ mm (the maximum value of the inter-electrode gap width for which the breakdown curves of the rf discharge have been recorded) at the turning point the condition $\nu_{en} \approx 8\omega$ holds.

The electron-drift-velocity values we have determined with our technique in hydrogen, argon and air are shown in figures 7–9. They are in good agreement with measured as well as calculated results of other authors [19, 40, 50, 52, 59, 60, 62, 68–77].

6. Conclusions

This paper contains the following results.

(i) A quite extensive historical survey of the work done in the fields of low-pressure gas breakdown and electron-drift-velocity determination is presented.

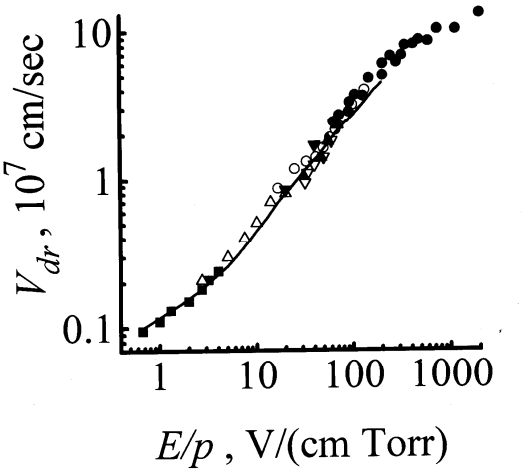

Figure 9. The electron-drift velocity in air against E/p: 1, our results and 2–7, other measured data (2 is from [69], 3 is from [40], 4 is from [72], 5 is from [73], 6 is from [74], 7 is from [75] and the curve is calculated in [76, 77]). Symbols have the same numbers as those in figure 7.

(ii) A lot of data on measuring breakdown curves of low-pressure rf discharges in argon, hydrogen and air with a broad range of inter-electrode gap widths and gas pressures are reported.

(iii) An analytical criterion for the gas breakdown in a combined (rf plus weak dc electrical fields) discharge is derived, including the anisotropy of the electrons' diffusion in the electrical field.

(iv) A novel technique for determining electron-drift velocities from the measured $U_{rf}(p)$ breakdown curves of a rf discharge is suggested. The electron-drift-velocity data for argon, hydrogen and air in the range $E/p =$ 50–2000 V cm^{-1} Torr^{-1} obtained with this technique are reported.

(v) Processes of the generation and loss of charged particles participating in the rf breakdown are discussed. The following branches of rf breakdown curves are proposed to be distinguished: multi-pactor, Paschen, diffusion–drift and emission-free ones.

References

[1] Moreau W M 1988 *Semiconductor Lithography: Principles, Practices, and Materials* (New York: Plenum)
[2] Flamm D L, Donnelly V M and Ibbotson D E 1983 *J. Vac. Sci. Technol.* B **1** 23
[3] Catherine Y and Couderc P 1986 *Thin Solid Films* **144** 265
[4] Yalamanchi R S and Thutupalli G K M 1988 *Thin Solid Films* **164** 103
[5] Raizer Yu P, Shneider M N and Yatsenko N A 1995 *Radio-Frequency Capacitive Discharges* (New York: CRC)
[6] Lisovskiy V A, Yegorenkov V D and Farenik V I 1995 *Record–Abstracts of the IEEE Int. Conf. on Plasma Science, Madison* p 162
[7] Lisovsky V A and Yegorenkov V D 1994 *J. Phys. D: Appl. Phys.* **27** 2340
[8] Gutton C, Mitra S K and Ylostalo V 1923 *C. R. Acad. Sci., Paris* **176** 1871
[9] Kirchner F 1925 *Ann. Phys., Lpz.* **77** 287

[10] Gutton C and Gutton H 1928 *C. R. Acad. Sci.* **186** 303
[11] Gutton H 1930 *Ann. Phys., Paris* **13** 62
[12] Gill E W B and Donaldson R H 1931 *Phil. Mag.* **12** 719
[13] Thomson J 1930 *Phil. Mag.* **10** 280
Thomson J 1934 *Phil. Mag.* **18** 696
Thomson J 1936 *Phil. Mag.* **21** 1057
Thomson J 1937 *Phil. Mag.* **23** 1
[14] Zouckermann R 1940 *Ann. Phys., Paris* **13** 78
[15] Githens S 1940 *Phys. Rev.* **57** 822
[16] Chenot M 1948 *Ann. Phys., Paris* **3** 277
[17] Hale D H 1948 *Phys. Rev.* **73** 1046
[18] Pim J A 1949 *Proc. IEE* P3 **96** 117
[19] Gill E B W and von Engel A 1949 *Proc. R. Soc.* A **197** 107
[20] Harries W L and von Engel A 1954 *Proc. R. Soc.* A **222** 490
[21] Francis G 1955 *Proc. Phys. Soc.* B **68** 137
[22] Kihara T 1952 *Rev. Mod. Phys.* **24** 45
[23] Salmon J 1955 *J. Phys. Radium* **16** 210
[24] Salmon J 1957 *Ann. Phys., Paris* **12** 827
[25] Sen S N and Ghosh A K 1962 *Ind. J. Phys.* **36** 605
[26] Levitskii S M 1957 *Zh. Tekh. Fiz.* **27** 970 (Engl. trans. 1958 *Sov. Phys. Tech. Phys.* **2** 887)
[27] Kropotov N Yu, Kachanov Yu A, Reuka A G, Lisovskiy V A, Yegorenkov V D and Farenik V I 1988 *Pis'ma Zh. Tekh. Fiz.* **14** 359 (Engl. trans. 1988 *Sov. Tech. Phys. Lett.* **14** 159)
[28] Kropotov N Yu, Lisovskiy V A, Kachanov Yu A, Yegorenkov V D and Farenik V I 1989 *Pis'ma Zh. Tekh. Fiz.* **15** (21) 17 (Engl. trans. 1989 *Sov. Tech. Phys. Lett.* **15** 836)
[29] Lisovskiy V A and Yegorenkov V D 1994 *Pis'ma Zh. Tekh. Fiz.* **20** (22) 68 (Engl. trans. 1994 *Tech. Phys. Lett.* **20** 920)
[30] Lisovskiy V A and Yegorenkov V D 1992 *Pis'ma Zh. Tekh. Fiz.* **18** (17) 66 (Engl. trans. 1992 *Sov. Tech. Phys. Lett.* **18** 572)
[31] Kirchner F 1947 *Phys. Rev.* **72** 348
[32] Varela A A 1947 *Phys. Rev.* **71** 124
[33] Sen S N and Bhattacharjee B 1965 *Can. J. Phys.* **43** 1543
[34] Sen S N and Bhattacharjee B 1966 *Can. J. Phys.* **44** 3270
[35] Kropotov N Yu, Lisovskiy V A and Farenik V I 1989 *Materialy 2 Vsesoyuznogo Soveshchaniya po vysokochastotnomy razryadu v volnovykh polyakh (Proc. 2 All Union Meeting on rf discharge in wave fields), Kuibyshev* p 11 (In Russian)
[36] Lisovskiy V A, Kropotov N Yu and Farenik V I 1996 *Pis'ma Zh. Tekh. Fiz.* **22** (24) 64 (Engl. trans. 1996 *Tech. Phys. Lett.* **22** 1029)
[37] Thompson B E and Sawin H H 1986 *J. Appl. Phys.* **60** 89
[38] Sato M and Shoji M 1997 *Japan. J. Appl. Phys.* **36** 5729
[39] Huxley L G H and Crompton R W 1974 *The Diffusion and Drift of Electrons in Gases* (New York: Wiley)
[40] Raether H 1964 *Electron Avalanches and Breakdown in Gases* (London: Butterworths)
[41] Howatson A M 1980 *An Introduction to Gas Discharges* (Oxford: Pergamon)
[42] Raizer Yu P 1991 *Gas Discharge Physics* (Berlin: Springer)
[43] Francis G 1960 *Ionization Phenomena in Gases* (London: Butterworths)
[44] Williams H B and Hatch A J 1953 *Phys. Rev.* **89** 339
[45] Hatch A J and Williams H B 1955 *Phys. Rev.* **100** 1228
[46] Noori M T and Harmon G S 1991 *J. Appl. Phys.* **69** 8052
[47] Hohn F, Jacob W, Beckmann R and Wilhelm R 1997 *Phys. Plasmas* **4** 940
[48] Lakshminarasimha C S and Lucas J 1977 *J. Phys. D: Appl. Phys.* **10** 313
[49] Tagashira H, Sakai Y and Sakamoto S 1977 *J. Phys. D: Appl. Phys.* **10** 1051
[50] Kucukarpaci H N and Lucas J 1981 *J. Phys. D: Appl. Phys.* **14** 2001
[51] Al-Amin S A J and Lucas J 1987 *J. Phys. D: Appl. Phys.* **20** 1590
[52] Nakamura Y and Kurachi M 1988 *J. Phys. D: Appl. Phys.* **21** 788
[53] Dall'Armi G, Brown K L, Purdie P H and Fletcher J 1992 *Aust. J. Phys.* **45** 185
[54] Wagner E B, Davis F J and Hurst G S 1967 *J. Chem. Phys.* **47** 3138
[55] Parker J H and Lowke J J 1969 *Phys. Rev.* **181** 290
[56] Lowke J J and Parker J H 1969 *Phys. Rev.* **181** 302
[57] Skullerud H R 1969 *J. Phys. B: At. Mol. Phys.* **2** 696
[58] Robson R E 1972 *Aust. J. Phys.* **25** 685
[59] Sakai Y, Tagashira H and Sakamoto S 1977 *J. Phys. D: Appl. Phys.* **10** 1035
[60] Saelee H T and Lucas J 1977 *J. Phys. D: Appl. Phys.* **10** 343
[61] Roznerski W 1978 *J. Phys. D: Appl. Phys.* **11** L197
[62] Blevin H A, Fletcher J and Hunter S R 1978 *J. Phys. D: Appl. Phys.* **11** 1653
Blevin H A, Fletcher J and Hunter S R 1978 *J. Phys. D: Appl. Phys.* **11** 2295
[63] Kitamori K, Tagashira H and Sakai Y 1980 *J. Phys. D: Appl. Phys.* **13** 535
[64] Roznerski W and Leja K 1980 *J. Phys. D: Appl. Phys.* **13** L181
[65] Puech V and Torchin L 1986 *J. Phys. D: Appl. Phys.* **19** 2309
[66] Suzuki M, Taniguchi T and Tagashira H 1990 *J. Phys. D: Appl. Phys.* **23** 842
[67] Abdulla R R, Dutton J and Williams A W 1981 *Proc XVth ICPIG, Minsk, Contributed Papers* vol 1, p 367
[68] Schlumbohm H 1965 *Z. Phys.* **182** 317
[69] Roznerski W and Leja K 1984 *J. Phys. D: Appl. Phys.* **17** 279
[70] Lowke J J 1963 *Aust. J. Phys.* **16** 115
[71] Jager G and Otto W 1962 *Z. Phys.* **169** 517
[72] Nielsen R A and Bradbury N E 1937 *Phys. Rev.* **51** 69
[73] Rees J A 1973 *Aust. J. Phys.* **26** 247
[74] Townsend J S 1925 *Motion of Electrons in Gases* (Oxford: Oxford University Press)
[75] Frommhold L 1964 *Fortschr. Phys.* **12** 597
[76] Lowke J J 1992 *J. Phys. D: Appl. Phys.* **25** 202
[77] Lowke J J and Morrow R 1995 *IEEE Trans. Plasma Sci.* **23** 661